Synthesis and Aggregation Behavior of Pluronic F127/Poly(lactic acid) Block Copolymers in Aqueous Solutions

X. Y. Xiong and K. C. Tam*

School of Mechanical & Production Engineering, Nanyang Technological University, 50 Nanyang Avenue, Singapore 639798

L. H. Gan

Natural Sciences, National Institute of Education, 1 Nanyang Walk, Singapore 639798

Received September 3, 2003; Revised Manuscript Received October 10, 2003

ABSTRACT: Poly(lactic acid) (PLA) were grafted to both ends of Pluronic F127 (PEO−PPO−PEO) to produce novel amphiphilic PLA-F127−PLA block copolymers. The aggregation behaviors of three different modified polymers were examined by laser light scattering and transmission electron microscopic techniques. The structure of aggregates produced from moderate to long PLA segments (PLAF127−29 (230 units of PLA) and PLAF127−48 (500 units of PLA) systems, respectively) was found to be normal bi-layer vesicles. Polymer with the shortest PLA segment (PLAF127−23 (142 units of PLA)) produces aggregates with complicated onion-like vesicles containing three layers. These vesicles possess microstructure similar to many biological systems, and they exhibit desirable properties for potential applications as drug delivery vehicles.

Introduction

Polymeric drug delivery systems have attracted increasing attention during the last two decades. Amphiphilic block copolymers have been widely studied due to their potential application in drug delivery system as they are capable of forming aggregates in aqueous solutions. These aggregates comprise of a hydrophobic core and hydrophilic shell. They are good vehicles for delivering hydrophobic drugs, since the drugs are protected from possible degradation by enzymes.[1−10] The morphology of nanoparticles produced from amphiphilic block copolymers can be varied by changing the composition of hydrophobic and hydrophilic blocks on the polymer chains. Various forms of morphologies have been reported, such as sphere, vesicles, rods, lamellas, tubes, large compound micelles, and large compound vesicles. Some of these structures are good candidates for drug delivery applications.[11−12]

Poly(ethylene oxide)−poly(propylene oxide)−poly(ethylene oxide) block copolymer (PEO−PPO−PEO) (Pluronics) is a macromolecular surfactant that has been extensively studied as a potential drug delivery vehicle due to its excellent biocompatibility.[5] The block copolymers are one of the very few synthetic polymeric materials approved by the U.S. Food and Drug Administration for use as food additives and pharmaceutical ingredients. The micelles produced from Pluronic block copolymers have been found to increase the oral and brain bioavailability of drugs and the efficacy of chemotherapeutic micelle formulation. In recent years, these systems have been evaluated as potential candidates in gene therapies and vaccination strategies.[13−23]

However, the critical micelle concentration (CMC) of Pluronic block copolymers is typically very high, because of the low hydrophobicity of PPO blocks. This limits the application of Pluronic micelles because they are not stable and are easily destroyed by dilution when injected into the human body. It is for this reason that chemical modifications of Pluronic block copolymers may be a necessary strategy to resolve this problem. For example, Pluronic copolymers had been hydrophobically modified with polycaprolactone (PCL). The modified block copolymer of PCL−Pluronic−PCL possessed a much lower CMC due to the hydrophobicity of PCL segments.[24,25] Bromberg et al. have grafted Pluronic with poly(acrylic acid) (PAA).[26−28] The gelation concentration of Pluronic-*g*-PAA copolymers is about 5−10 times lower than that of Pluronic. Only one paper on the synthesis of PLA−Pluronic−PLA was reported, where copolymer films were examined for potential applications as adhesive-prevention membranes.[29] Apart from these few studies, not much research has been conducted on the chemical modification of Pluronic block copolymers.

In this paper, hydrophobic PLA chains were grafted on both ends of Pluronic F127, yielding PLA-F127−PLA block copolymers. Some of the reasons for selecting PLA are (a) it is a biodegradable and biocompatible polyester and (b) it can enhance the hydrophobicity of modified Pluronic copolymers, thereby lowering the CMC value. The PLA-F127−PLA block copolymers possess excellent biocompatibility because of the Pluronic and PLA segments. In addition, the biodegradability of PLA blocks makes it attractive for use in controlled drug release systems because the release rates can be controlled by varying the length and degradation rate of PLA blocks.

Experimental Section

Materials. Pluronic F127 were kindly supplied by BASF Corporation (Mount Olive, NJ) and dried overnight under vacuum before use. L-Lactide was purchased from Aldrich and recrystallized from ethyl acetate (EtAc). The purified L-lactide was stored at 4−5 °C under argon environment. Stannous octoate ($Sn(Oct)_2$) was purchased from Aldrich and used as received. Osmium tetroxide (OsO_4) in 2-methyl-2-propanol (2.5 wt %) needed for staining purposes was purchased from Aldrich and used as received.

* To whom correspondence should be addressed. E-mail: mkctam@ntu.edu.sg.

10.1021/ma035292d CCC: $25.00
Published on Web 11/26/2003

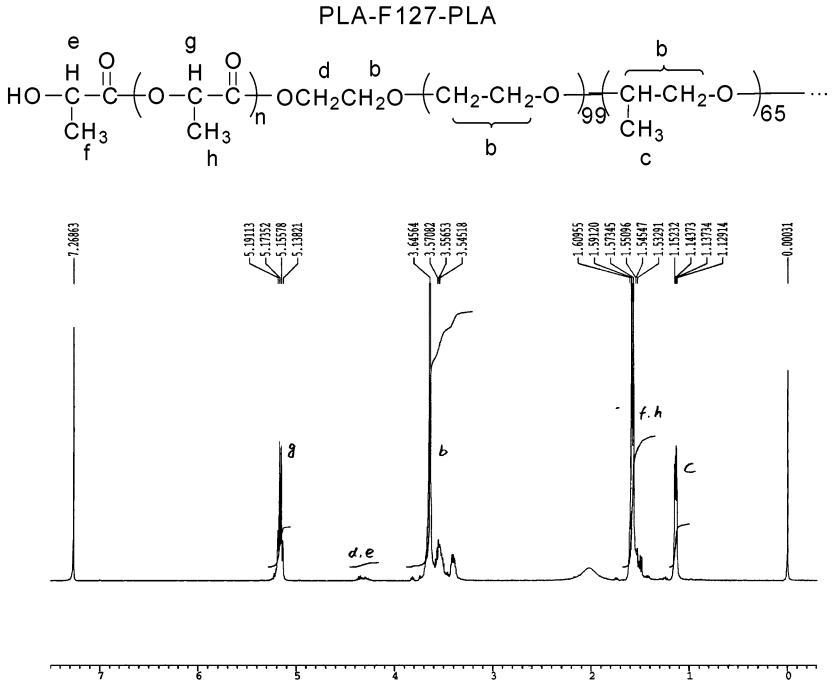

Figure 1. ^{1}H NMR spectrum of PLAF127−29 ($CDCl_3$).

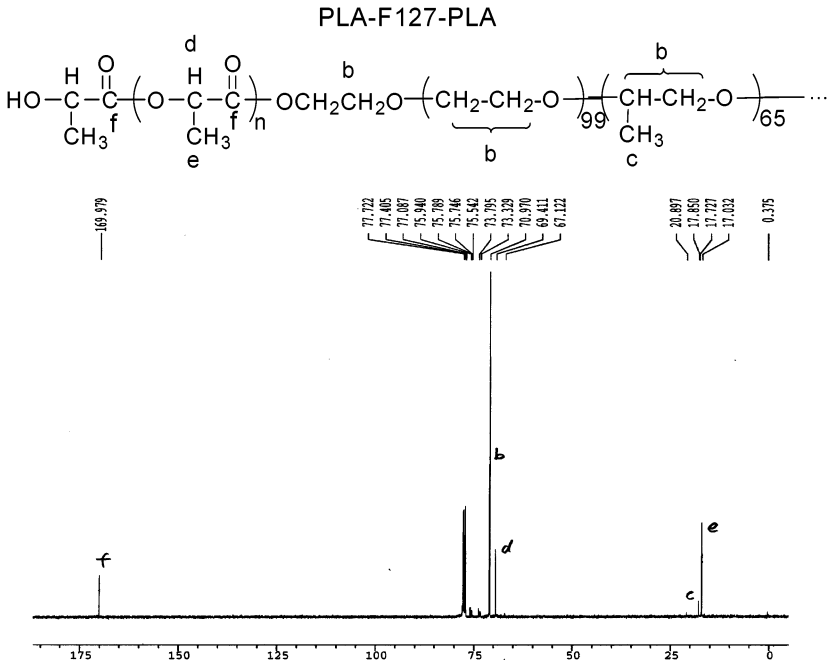

Figure 2. ^{13}C NMR spectrum of PLAF127−29 ($CDCl_3$).

Synthesis of PLA-F127−PLA Block Copolymers. PLA segments were attached to both ends of Pluronic F127 copolymers to obtain amphiphilic block copolymers of PLA-F127−PLA. The synthesis procedure of a typical PLAF127−29 system is as follows. A round-bottom flask with a stopcock was heated under reduced pressure to remove the moisture. After cooling to room temperature, argon was introduced into the flask. Following this, L-lactide (86.6 mmol) and Pluronic F127 (0.50 mmol) were added, and the mixture was heated with continuous stirring to produce a well-mixed molten phase. The mixture was then cooled, and $Sn(Oct)_2$ (0.1 wt % of L-lactide) was added to the flask under argon environment. The mixture was degassed by six vacuum-purge cycles and then heated to 180 °C. After stirring for 15 h, the content was cooled to room temperature. The product was dissolved in methylene chloride and then precipitated twice in 10-fold volume of methanol and once in 10-fold volume of diethyl ether. The polymer designated PLAF127−29 was filtered and dried overnight under vacuum. The polymer powder was obtained with a 80% yield. ^{1}H NMR (400 MHz, $CDCl_3$, TMS), δ (ppm); 1.13−1.15 (m, $-OCH_2-CH(CH_3)-$), 1.54−1.63 (m, $-O-CH(CH_3)-CO-$ and $HO-CH(CH_3)-CO-$), 3.35−3.75 (m, $-OCH_2-$ CH_2- and $-OCH_2-CH(CH_3)-$), 4.25−4.35 (m, $HO-CH(CH_3)-CO-$ and $-CO-OCH_2-CH_2-O-$), 5.15−5.19 (m, $-O-CH(CH_3)-CO-$) (Figure 1). ^{13}C NMR (400 MHz, $CDCl_3$), δ (ppm): 17.03 ($-O-CH(CH_3)-CO-$), 17.85 ($-OCH_2-CH(CH_3)-$), 69.41 ($-O-CH(CH_3)-CO-$), 70.97 ($-OCH_2-CH_2-$ and $-OCH_2-CH(CH_3)-$), 169.98 ($-O-CH(CH_3)-CO-$) (Figure 2). Two additional PLA-F127−PLA copolymers with different block composition were similarly synthesized. They were designated as PLAF127−23 and PLAF127−48. In the designation for the three polymers PLAF127−23, 29, and 48, the numeric numbers 23, 29, and 48 correspond to the molecular weight in kDa, determined from NMR.

Sample Preparation. The aggregates of PLA-F127−PLA in aqueous solutions were prepared as follows: PLA-F127−PLA block copolymers were initially dissolved in tetrahydrofuran (THF). The PLA-F127−PLA solutions were added dropwise to distilled water under gentle stirring, after which THF was removed under reduced pressure.

Characterization. Nuclear magnetic resonance (NMR) spectra were recorded at room temperature using a Bruker ACF-400 (400 MHz) Fourier transform spectrometer. Chemical shifts (δ) were given in ppm using tetramethylsilane (TMS) as an internal reference. GPC of the copolymers was performed on an Agilent 1100 apparatus (Germany) equipped with a differential refractometer as the detector. Tetrahydrofuran (THF) was used as the mobile phase with a flow rate of 1.0 mL/min. The CMC was measured using a Dataphysics DCAT-21 tensiometer.

Laser Light Scattering (LLS). *Static Light Scattering.* Static light scattering (SLS) was used to measure and analyze the time-average scattered intensities. The method is often used to determine microscopic properties of particles such as the *z*-average radius of gyration (R_g), the weight-average molecular weight ($\bar{M}_w$), and the second virial coefficient (A_2) according to eq 1

$$\frac{KC}{R_\theta} = \frac{1}{M_w}\left[1 + \frac{16\pi^2 n^2 \langle R_g^2\rangle \sin^2\left(\frac{\theta}{2}\right)}{3\lambda^2}\right] + 2A_2C \qquad (1)$$

where, the Rayleigh ratio, $R_\theta = (I_s r^2/I_i \sin\theta)$; $K = [4\pi^2 n^2(\partial n/\partial C)^2/(N_A\lambda^4)]$; C is the concentration of the polymer solution; n is the refractive index of the solvent; θ is the angle of measurement; λ is the wavelength of laser light; N_A is Avogadro's constant; and $(\partial n/\partial C)$ is the refractive index increment of the polymer solution. A plot of (KC/R_θ) versus $[\sin^2(\theta/2) + kC]$ (where k is a plotting constant) can be used to determine the molecular parameters. By extrapolating the data to zero angles and concentrations, R_g and A_2 can be obtained from the slopes, respectively. A simultaneous extrapolation to zero angle and concentration yields an intercept, which is the inverse of the $\bar{M}_w$.

Dynamic Light Scattering. The frequency of scattered light fluctuates around the incident light due to the constant motion of the polymer molecules. Dynamic light scattering (DLS) measures the intensity fluctuations with time and correlates these fluctuations to the properties of the scattering objects. In general, the terms of correlation functions of dynamic variables are always used to describe the response of the scattering molecules to the incident light. From the expression

$$\Gamma = Dq^2 \qquad (2)$$

the translational diffusion coefficients, D, can be determined. Γ is the decay rate, which is the inverse of the relaxation time, τ; q *is* the scattering vector ($q = (4\pi n \sin(\theta/2))/\lambda$), where θ is the scattering angle, n is the refractive index of the solution, and λ is the wavelength of the incident light. If the Stokes−Einstein equation is used, the apparent hydrodynamic radius, R_h, can be calculated using the following equation:

$$R_h = \frac{kT}{6\pi\eta D} \qquad (3)$$

where k is the Boltzmann constant; T is the absolute temperature; and η is the solvent viscosity.

A Brookhaven BIS200 laser scattering system was used to perform the static and dynamic light scattering experiments. The light source is a power adjustable vertically polarized 350 mW argon ion laser with a wavelength of 488 nm. The inverse Laplace transform of REPES supplied with the GENDIST software package was used to analyze the time correlation function (TCF), and the probability of reject was set to 0.5.

Transmission Electron Microscope (TEM). TEM was performed on a JEOL JEM-2010 electron microscope at an acceleration voltage of 200 kV. A copper grid (400 meshes) with a carbon film was used. The copper grid was immersed in a drop of the aqueous polymer solution for 2 min and then removed and dried. A drop of osmium tetroxide (OsO_4) in 2-methyl-2-propanol (2.5 wt %) was placed on the copper grid for 2 min. The copper grid was then dried overnight at room temperature prior to measurement.

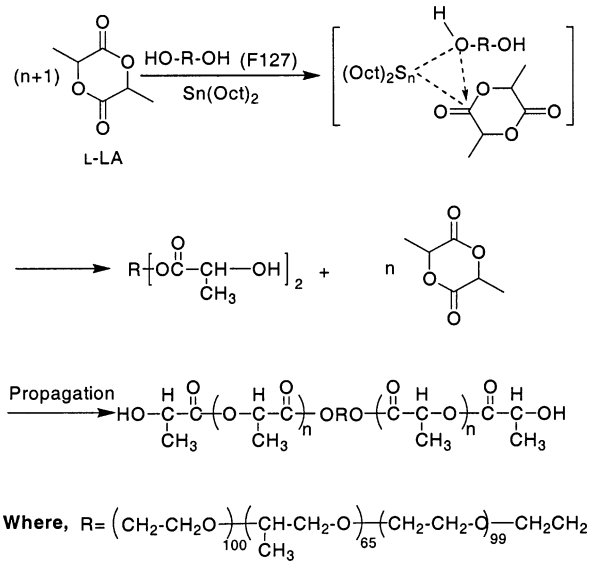

Figure 3. Synthesis mechanism of PLA-F127−PLA block copolymers.

Results and Discussion

The block copolymers PLA-F127−PLA were synthesized by ring opening polymerization of the monomer L-lactide using Pluronic copolymer F127 as the initiator and stannous octoate ($Sn(Oct)_2$) as the catalyst. The mechanism of the reaction is that of coordination polymerization (Figure 3).[30,31] Many other catalysts such as SnO, SnO_2, Ab_2O_3, and PbO have been used in the synthesis of PEO/PCL and PEO/PLA block copolymers.[32,33] However, $Sn(Oct)_2$ appears to have the advantage of producing a polymer of higher molecular weight with better yield.[34] It is important to note that the amount of $Sn(Oct)_2$ added has a significant effect on the polymer produced. At low $Sn(Oct)_2$ concentration, the polymer obtained has a narrower polydispersity index (PDI). However, an insufficient amount of $Sn(Oct)_2$ would lead to failure in the polymerization. It was found that an optimum amount of $Sn(Oct)_2$ is around 0.1 wt % of the monomer.

The polymer composition, structure, and molecular weight were characterized by NMR and GPC techniques. Figure 1 shows a ^1H NMR spectrum of a typical PLA-F127−PLA in $CDCl_3$. The small peak at δ of 4.30 ppm belongs to methylene protons of the PLA-CO−OCH_2−CH_2−O−F127 segment, indicating the successful synthesis of the PLA-F127−PLA block copolymer. The absence of a peak at δ of 4.9−5.0 ppm which could have been contributed by the methine proton of the PLA-O−CH(CH_3)-COOH group, suggests that there was negligible or no PLA homopolymer in the PLA-F127−PLA block copolymer.[33,34] The degree of polymerization (n) of PLA in PLA_n-F127−PLA_n copolymers was calculated from the peak intensity ratio of methyl protons of PLA (O−CH(CH_3)−CO−: δ = 1.58 ppm) and methyl protons of F127 (−OCH_2−CH(CH_3)−: δ = 1.15 ppm). The number-average molecular weight ($\bar{M}_n$) of the PLA_n-F127−PLA_n copolymer was obtained using the following expression:

Table 1. Characterization of PLA-F127−PLA Block Copolymers

sample	W_{LA}% in feed	W_{LA}%[a] in product	unit ratio for PLA:PEO:PPO	$\bar{M}_n$ (theory)	$\bar{M}_n$ (NMR)	$\bar{M}_w/\bar{M}_n$ (GPC)	$\bar{M}_w$[b]	yield (%)
PLAF127−23	50	44.7	142:200:65	25 200	22 800	1.34	30 600	85
PLAF127−29	66.7	57.2	230:200:65	37 800	29 000	1.54	44 700	80
PLAF127−48	80	73.8	500:200:65	50 400	48 000	1.41	67 700	82.5

[a] Determined by the integration ratio of the peak at 1.58 ppm (−O−CH(CH_3)−CO− group in PLA block) and the peak at 1.15 ppm (−OCH_2−CH(CH_3)− group in Pluronic F127 block) in the ^{1}H NMR spectrum. [b] $\bar{M}_w = \bar{M}_n$ (NMR) × [$\bar{M}_w/\bar{M}_n$ (GPC)].

$$\bar{M}_n = \bar{M}_n(\text{F127}) + 144n \quad (4)$$

The calculated molecular weight contents of PLA in PLAF127−23, PLAF127−29, and PLAF127−48 block copolymers are in good agreement with the PLA contents in the synthesis composition (Table 1).

The ^{13}C NMR spectrum of a typical PLA-F127−PLA in $CDCl_3$ is shown in Figure 2. The peaks at 17.03, 69.41, and 169.98 ppm are related to the PLA block. The peaks at 17.85 and 70.97 ppm belong to the F127 segments.Figure 4 shows the GPC trace of PLAF127−48 block copolymer. The PDI of PLAF127−23, PLAF127−29, and PLAF127−48 block copolymers were determined by GPC measurements (Table 1).

The aggregation behavior of PLA-F127−PLA block copolymers in aqueous solutions was studied by static and dynamic light scattering. The concentration used in the laser light scattering study is much lower than 0.5 wt % because the overlap concentration, defined by $C^* = 1/[\eta]$, is ∼ 0.5 wt %. The behavior of individual particles can be characterized at this concentration.[35]

The Zimm plot (described by eq 1) of PLAF127−48 is shown in Figure 5. Table 2 summarizes the values of R_g, $\bar{M}_w$, and the aggregation numbers for PLAF127−23, PLAF127−29, and PLAF127−48.

The dynamics of PLA-F127−PLA block copolymers in aqueous solution can be successfully examined by DLS. Figure 6 shows the relaxation time distribution functions of PLAF127−23, PLAF127−29, and PLAF127−48 block copolymers in aqueous solutions at different scattering angles.

One single peak was observed, and the peak relaxation times shifted to lower values with increasing angles, suggesting that only one type of particle was present. The relaxation rate Γ (the reciprocal of peak relaxation time) was found to be proportional to the square of the scattering vector (q^2), confirming that the scattering objects are related to translational diffusion. The hydrodynamic radii R_h of the micelles determined from eq 3 for PLAF127−23, PLAF127−29, and PLAF127−48 are 50, 56, and 56 nm, respectively (Table 2), which indicates that the aggregate size increases marginally with increasing PLA block length. The R_g/R_h values of the three copolymers are all larger than that predicted for a nondraining hard sphere (0.774) (Table 2).

To confirm the structures of the PLAF127−23, PLAF127−29, and PLAF127−48 aggregates in aqueous solutions, samples were examined by TEM. The hydrophobic PLA segments containing double bonds were stained with OsO_4, and the TEM micrographs of PLAF127−23, PLAF127−29, and PLAF127−48 aggregates are shown in Figure 7a−c.

TEM micrographs revealed that the structures of PLAF127−29 and PLAF127−48 aggregates are those of vesicle with a diameter of about 80 nm for PLAF127−29 (Figure 7b) and 100 nm for PLAF127−48 (Figure 7c). The thickness of the hydrophobic layer is approximately

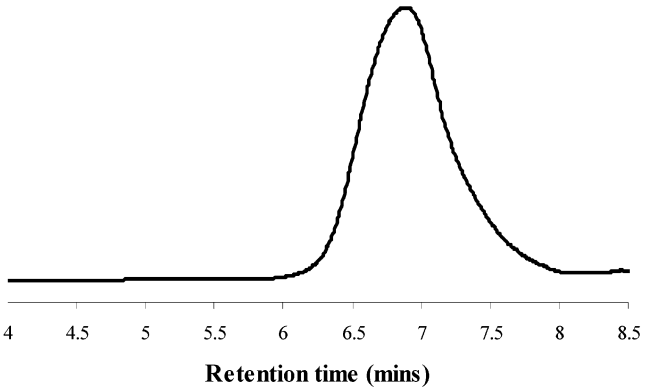

Figure 4. GPC trace of PLAF127−48 block copolymer (RI signal).

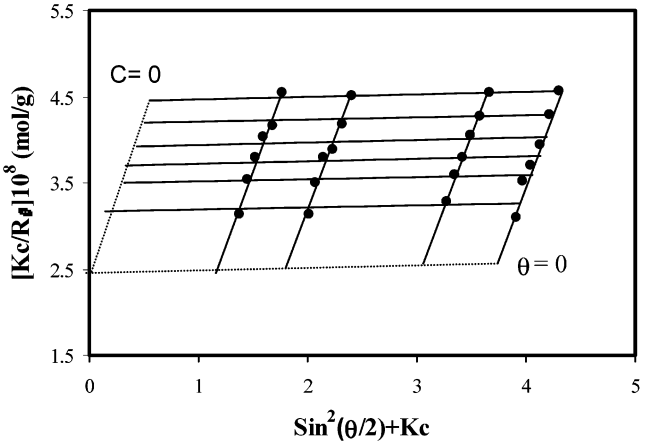

Figure 5. Zimm plot of aggregates formed from PLAF127−48 block copolymer in aqueous solution at room temperature, where the concentration range was from 0.01 to 0.06 mg/mL.

Table 2. Laser Light Scattering Results of PLA-F127−PLA Block Copolymers at Aqueous Solutions at Room Temperature

sample	R_h (nm)	R_g (nm)	R_g/R_h	$\bar{M}_w$ (aggregates)	$N_{aggretation}$[a]
PLAF127−23	50	95	1.9	3.9×10^7	1.3×10^3
PLAF127−29	56	56	1.0	4.4×10^7	9.9×10^2
PLAF127−48	56	48	0.85	3.3×10^7	4.8×10^2

[a] $N_{aggregation} = \bar{M}_w$(aggregates)/$\bar{M}_w$(polymer), where $\bar{M}_w$(polymer) is shown in Table 1.

5−10 nm. The size distribution of PLAF127−48 aggregates is broader. However, PLAF127−23 aggregates (diameter of ∼100 nm) have the appearance of onion-like vesicles with three layers (Figure 7a). The thickness of the outside hydrophobic layer is about 5−10 nm and the radius of the internal hydrophobic core is about 30 nm (Figure 7a). Based on these results, we proposed two possible microstructures, which are schematically illustrated in parts a and b of Figure 8.

The particle size and the morphology determined from TEM studies are consistent with the results derived

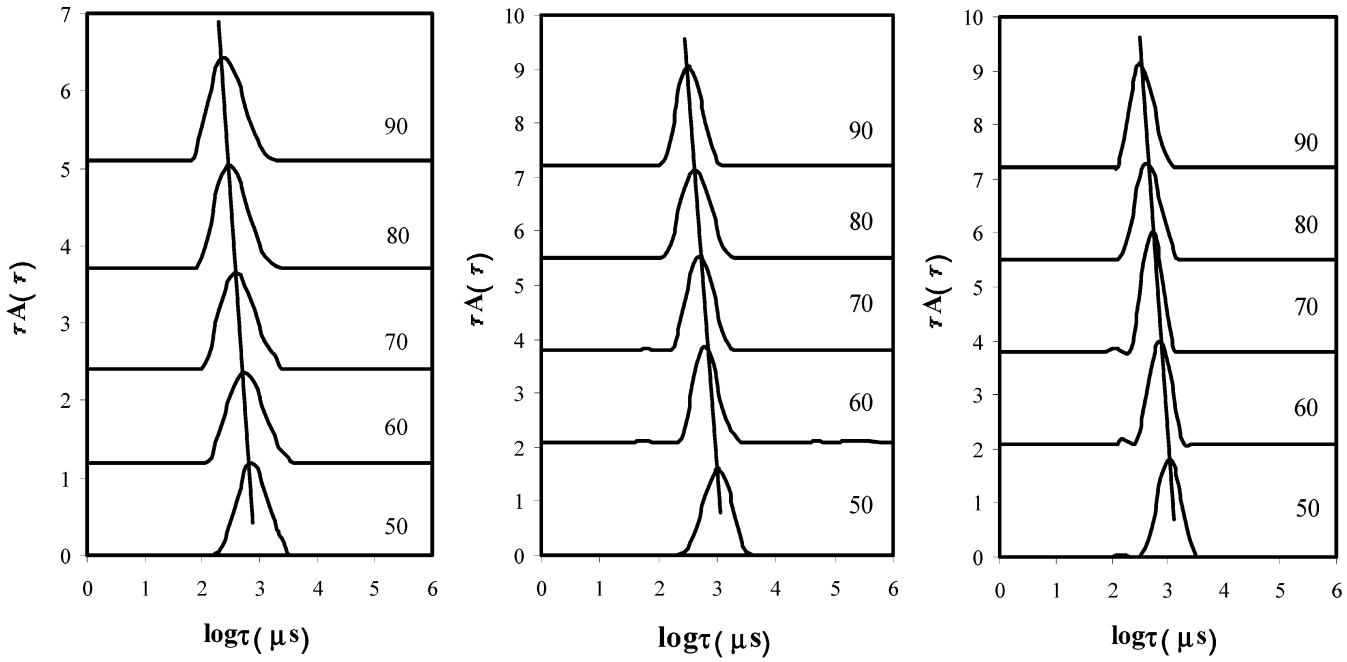

Figure 6. Relaxation time distribution functions of PLAF127−23 (A, 0.01 wt %), PLAF127−29 (B, 0.01 wt %), and PLAF127−48 (C, 0.006 wt %) block copolymers in aqueous solutions at different scattering angles.

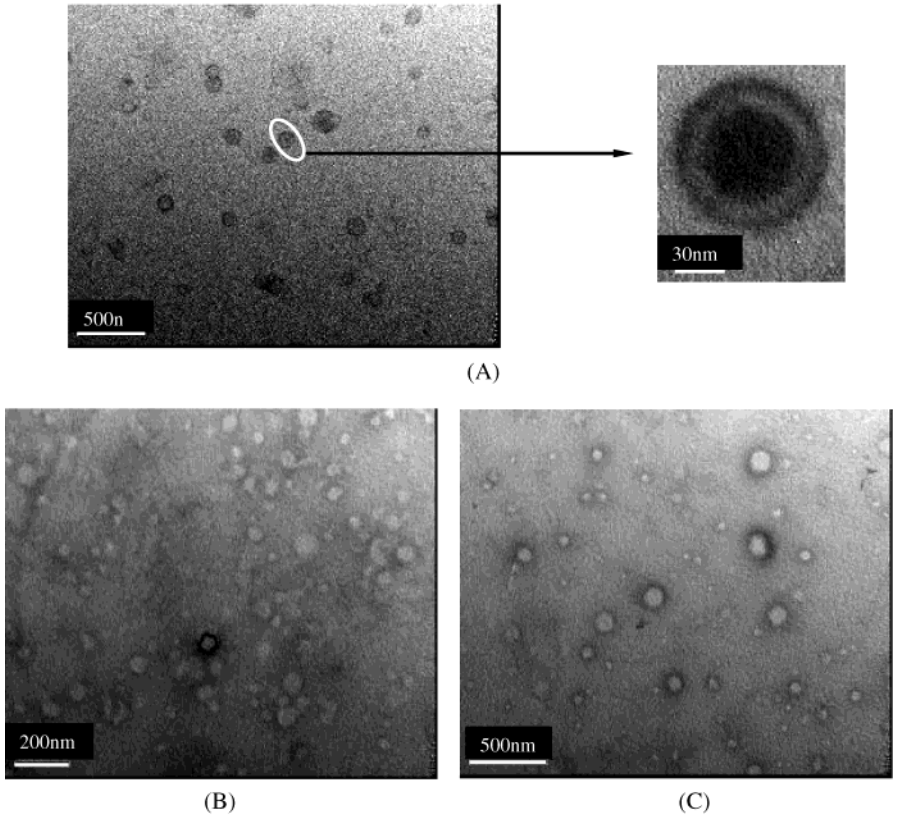

Figure 7. TEM micrographs of aggregates formed from PLAF127−23 (a), PLAF127−29 (b), and PLAF127−48 (c) block copolymers in water.

from LLS data. The reason that the structure of PLAF127−23 aggregates is different from that of PLAF127−29 and PLAF127−48 is most likely related to the length of PLA segments. The hydrophobic−hydrophilic balance of the copolymer is inadequate to form normal bi-layer vesicles; thus, more complex onion-like vesicle containing additional polymer chains are produced.

The effect of the concentration of the PLAF127−48 block copolymer in aqueous solutions on the particle size is shown in Figure 9. The relaxation time peak of the copolymers at different concentrations is identical, indicating that the particles size of PLAF127−48 is independent of polymer concentration. This confirms that the aggregation mechanism of the two polymers corresponds to the closed association model.

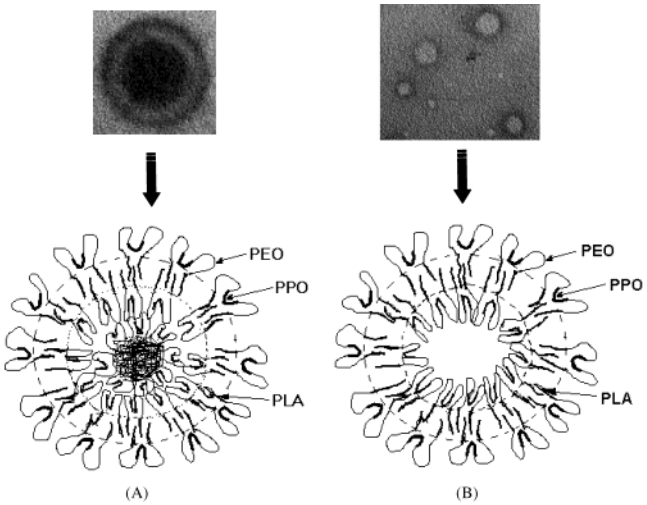

Figure 8. Possible microstructure of vesicles formed from PLA-F127−PLA block copolymers in aqueous solution: (a) onion-like vesicles from PLAF127−23; (b) bilayer vesicles from PLAF127−29 and PLAF127−48.

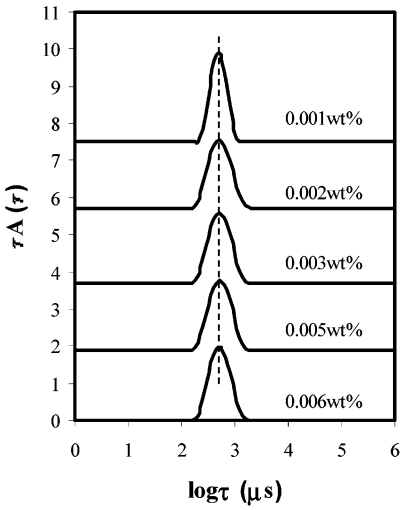

Figure 9. Relaxation time distribution functions of PLAF127−48 in aqueous solutions with different concentrations at a scattering angle of 90°.

The CMC values of PLA-F127−PLA block copolymers were determined by surface tension measurements. The surface tension of the PLAF127−23, PLAF127−29, and PLAF127−48 aggregates was plotted against the polymer concentration (Figure 10), and the CMC values of the PLAF127−23, PLAF127−29, and PLAF127−48 block copolymers were determined to be 2.43×10^{-5}, 1.80×10^{-5}, and 2.27×10^{-6} wt %, respectively. It is evident that the CMC decreases with increasing PLA block length, because the hydrophobicity of the PLA-F127−PLA polymers is increased. The extremely low CMC values of these modified Pluronic polymers augur well for their potential applications as vehicles for drug delivery. These aggregates comprising different kind of vesicles are potential candidates for enhanced drug delivery applications because they can be used to deliver both hydrophobic and hydrophilic drugs. In addition, the size of PLA-F127−PLA aggregates is ideal for such applications as we can achieve better circulation time and bioavailability of the aggregates in biological system. For drug delivery applications, the preferred range of particle size is ~10 to 100 nm, and the size of PLA-F127−PLA aggregates lie within this range.[15] Diffusional studies on the drug release behavior of PLA-F127−PLA block copolymers in aqueous environment is currently in progress.

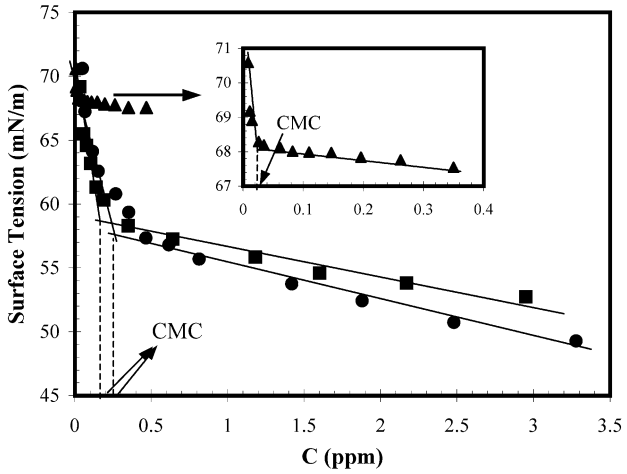

Figure 10. Surface tension as a function of concentrations of PLAF127−23 (●), PLAF127−29 (■), and PLAF127−48 (▲) block copolymers in aqueous solutions at room temperature.

Conclusions

Three different PLA-F127−PLA block copolymers have been synthesized. The aggregation behaviors of the block copolymers in aqueous solutions were studied in detail by LLS and TEM. The diameter of PLA-F127−PLA aggregates was around 100 nm. The structures of aggregates for PLAF127−29 were found to be bi-layer vesicles, whereas for PLAF127−23, a more complicated onion-like vesicle was postulated. These systems are believed to have potentials as vehicles for drug delivery applications.

Acknowledgment. We acknowledge the financial support in the form of a SDS grant from the school of MPE. X.Y.X. would like to thank NTU for the financial support in the form of a Ph.D. graduate scholarship.

References and Notes

(1) Bae, Y. H.; Huh, K. M.; Kim, Y.; Park, K. H. *J. Controlled Release* **2000**, *64*, 3−13.
(2) Gan, Z. H.; Jim, T. F.; Li, M.; Yuer, Z.; Wang, S. G.; Wu, C. *Macromolecules* **1999**, *32*, 590−594.
(3) Ge, H. X.; Hu, Y.; Jiang, X. Q. *J Pharm. Sci.* **2002**, *91*, 1463−1473.
(4) Kositza, M. J.; Bohne, C.; Alexandridis, P.; Hatton, T. A.; Holzwarth, J. F. *Macromolecules* **1999**, *32*, 5539−5551.
(5) Lee, S. H.; Kim, S. H.; Kim, Y. H. *Macromol. Res.* **2002**, *10*, 85−90.
(6) Wu, C.; Liu, T.; Chu, B.; Schneider, D. K.; Graziano, V. *Macromolecules* **1997**, *30*, 4574−4583.
(7) Yekta, A.; Xu, B.; Duhamel, J.; Adiwidjaja, H.; Winnik, M. A. *Macromolecules* **1995**, *28*, 956−966.
(8) Yuan, M. L.; Wang, Y. H.; Li, X. H.; Xiong, C. D.; Deng, X. M. *Macromolecules* **2000**, *33*, 1613−1617.
(9) Zhao, Y.; Liang, H. J.; Wang, S. G.; Wu, C. *J. Phys. Chem. B* **2001**, *105*, 848−851.
(10) Rosler, A.; Vandermeulen, G. W. M.; Klok, H. A. *Adv. Drug Delivery Rev.* **2001**, *53*, 95−108.
(11) Discher, D. E.; Eisenberg, A. *Science* **2002**, *297*, 967−973.
(12) Yu, K.; Bartels, C.; Eisenberg, A. *Macromolecules* **1998**, *31*, 9399−9402.
(13) Alexandridis, P.; Hatton, T. A. *Colloids Surf.* **1995**, *96*, 1−46.
(14) Kabanov, A. V.; Batrakova, E. V.; Alakhov, V. Y. *Adv. Drug Delivery Rev.* **2002**, *54*, 759−779.
(15) Kabanov, A. V.; Batrakova, E. V.; Alakhov, V. Y. *J. Controlled Release* **2002**, *82*, 189−212.
(16) Bohorquez, M.; Koch, D.; Trygstad, T.; Pandit, N. *J. Colloid Interface Sci.* **1999**, *216*, 34−40.

(17) Pedersen, J. S.; Gerstenberg, M. C. *Colloid Surf. A* **2003**, *213*, 175−187.
(18) DesNoyer, J. R.; McHugh, A. J. *J. Controlled Release* **2003**, *86*, 15−24.
(19) Su, Y. L.; Wang, J.; Liu, H. Z. *Macromolecules* **2002**, *35*, 6426−6431.
(20) Kozlov, M. Y.; Melik-Nubarov, N. S.; Batrakova, E. V.; Kabanov, A. V. *Macromolecules* **2000**, *33*, 3305−3313.
(21) Caragheorgheopol, A.; Schlick, S. *Macromolecules* **1998**, *31*, 7736−7745.
(22) Thurn, T.; Couderc-Azouani, S.; Bloor, D. M.; Hozwarth, J. F.; Wyn-Jones, E. *Langmuir* **2003**, *19*, 4363−4370.
(23) Svingen, R.; Alexandridis, P.; Akerman, B. *Langmuir* **2002**, *18*, 8616−8619.
(24) Ha, J. C.; Kim, S. Y.; Lee, Y. M. *J. Controlled Release* **1999**, *62*, 381−392.
(25) Kim, S. Y.; Ha, J. C.; Lee, Y. M. *J. Controlled Release* **2000**, *65*, 345−358.
(26) Bromberg, L. *Ind. Eng. Chem. Res.* **1998**, *37*, 4267−4274.
(27) Bromberg, L. *Langmuir* **1998**,. *14*, 5806−5812.
(28) Bromberg, L. *Macromolecules* **1998**, *31*, 6148−6156.
(29) Yamaoka, T.; Takahashi, Y.; Fujisato, T.; Lee, C. W.; Tsuji, T.; Ohta, T.; Murakami, A.; Kimura, Y. *J. Biomed. Mater. Res.* **2001**, 54, 470−479.
(30) Kricheldorf, H. R.; Krerser-Saunders, I.; Boettcher, C. *Polymer* **1995**, *35*, 219.
(31) Kricheldorf, H. R.; Krerser-Saunders, I.; Stricker, A. *Macromolecules* **2000**, *33*, 702−709.
(32) Xie, W. H., Chen, D. P., Fan, X. H., Li, J., Wang, P. G.; Cheng, H. N.; Nickol, R. G. *J. Polym. Sci. Part A: Polym. Chem.* **1999**, *37*, 3486−3491.
(33) Rashkov, I.; Manolova, N.; Li, S. M.; Esplartero, J. L.; Vert, M. *Macromolecules* **1996**, *29*, 50−56.
(34) Li, S. M.; Esplartero, J. L.; Manolova, N.; Vert, M. *Macromolecules* **1996**, *29*, 57−62.
(35) Dai, S.; Tam, K. C.; Jenkins, R. D. *Macromolecules* **2000**, *33*, 7021−7028.

MA035292D